Dynamic Displacement Self-Sensing and Robust Control of Cantilever Piezoelectric Actuators Dedicated for Microassembly

Micky Rakotondrabe, *Member, IEEE,* Ioan Alexandru Ivan, *Member, IEEE*, Sofiane Khadraoui, Cedric Clevy, Philippe Lutz, *Member, IEEE*, and Nicolas Chaillet, *Member, IEEE*

***Abstract*— The main objective of this paper is the dynamic self-sensing of the motion of piezoelectric actuators. The proposed measurement technique is afterwards used for a closed-loop control.**

Aiming to obtain a self-sensing scheme that estimates the transient and steady-state modes of the displacement, we extend a previous static self-sensing scheme by adding a dynamic part. Analytical solutions are provided to compute the gains of this dynamic part. Afterwards, the proposed dynamic self-sensing result is used in a closed-loop control. The experimental results demonstrate the concept and evaluate the accuracy and the efficiency of the proposed technique for closed-loop applications.

I. Introduction

Micromanipulation and microassembly usually require the positioning and trajectory control of microrobots with an accuracy that can be in the range of up to several tens of nanometers. Such accuracy is required for applications like biomedical (cell or biomolecule manipulation, pharmacy) but also for assembling microsystems for telecommunications and sensors technologies domains [1]. To reach such performances, active materials like piezoelectric ones (widespread for applications at the micro scale) are used. Nevertheless their complexity and nonlinear behavior limit their development and use [2]. This is why control techniques are systematically used to improve the performances of these materials and systems.

At the microscale, open loop control methods show interesting results but they do not efficiently enable the rejection of the environmental condition influences [3]. Alternately, closed loop control techniques offer good results but require the integration of expensive sensors able to provide a very good measurement resolution with a fair noise level and a good stability [4]. Such sensors are often bulky (laser interferometers or triangulation sensors, AFMs etc.) making them non-embarkable and too complex for integration into small systems. Thus, it is really difficult to find the good compromise between the available free space and desired performances [5][6].

Promising approaches avoiding external sensors in meso and micro systems are called self-sensing methods. They allow both actuation and sensing capabilites, and are especially (but not necessarily) based on piezoelectric materials. Given the reversibility of piezoelectric effect, self-sensing does or should not influence the actuation capabilities in terms of range or dynamics. It could provide simultaneous quantitative information of end-effector displacement, manipulation force, close contact detection or even temperature evaluation.

The piezoelectric self-sensing method was mainly developed for vibration control [7] or usually offered short-term measurements (measurement rarely available for more than 5 seconds) [8]. Hence, it could not be applied for micromanipulation or microassembly tasks. Indeed, such applications require the combination of dynamic and static sensing with duration from several tens of seconds to several minutes (duration of the transport of a micro-object). Moreover, very few works refer to the use of self-sensing method for the control of positioning [9]. In our previous works [10] [11], a new scheme of self-sensing has been proposed for measuring the displacement in its steady-state for more than 600s. Unfortunately, the static self sensing technique presented in [10] is not convenient for control loops faster than 0.2 seconds. The core of the present paper is to extend the previous static self-sensing technique to dynamic self-sensing. Afterwards, the estimated displacement of the piezoelectric actuator (through the self-sensing) is integrated in a feedback H_∞ control. This technique is used due to its robustness and the account of the specifications like performances and disturbance rejection. Such performances guarantee is very useful in the control of small systems where the sensitivity to environmental disturbances is very high and the model is prone to uncertainties [4].

Section II of the paper briefly reminds the basics of the static self-sensing, according to our previous works [10] and [11]. In section III, we present the extension to dynamic self-sensing. Section IV is dedicated to the controller synthesis and experimental results evaluation. Finally, section V gives the concluding remarks.

This work was supported by the EU FP7-SP3-People Program under Grant No: PIEF-GA-2008-219412 (New Micro-Robotic Systems featuring Piezoelectric Adaptive MicroStructures for Sensing and Actuating, with Associated Embedded Control: MicroPAdS).

Authors are with the FEMTO-ST Institute, AS2M Department, 24 Rue Alain Savary, 25000 Besancon, France (phone: +33-381-402-803; fax: +333-381-853-998; e-mail: {mrakoton, alex.ivan, sofiane.khadraoui, cclevy, plutz, nicolas.chaillet}@ femto-st.fr).

II. PRINCIPLE OF THE STATIC SELF-SENSING OF THE DISPLACEMENT

In this section, we remind the quasi-static self-sensing principle as proposed in our previous work [10]. By "static" we refer to any signal operating at a frequency significantly lower (10 to 100 times) than the first resonance mode of the actuator.

A. Principle scheme

Consider a unimorph cantilevered beam piezoactuator (piezocantilever), made up of a passive layer and a piezo-layer, subjected to an electrical excitation V_{in} (Fig.1).

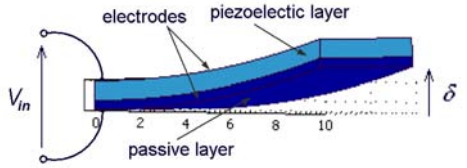

Figure 1. A unimorph piezocantilever subjected to an electrical voltage.

In the absence of an external sensor, it is still possible to estimate the displacement δ by measuring the amount of electric charge Q transferred to the electrodes by the known input signal V_{in}. For that, two steps are achieved. First, an electronic circuit (charge integrator) based on operational amplifiers is used to measure the charge by providing an output voltage V_{out}. Afterwards, an estimator based on the actuator and the electronic circuit models is implemented on a computer or a real-time controller (Fig.2). The estimator provides the estimated displacement $\hat{\delta}_s$ of the real displacement δ in its steady-state and low frequency mode (Fig.3 - dotted curve).

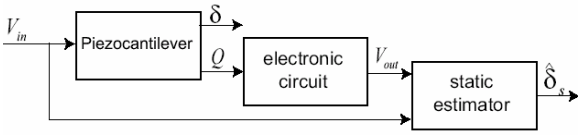

Figure 2. Principle scheme of the static self-sensing technique.

B. Governing equation

Assuming that the bias current of the electronic circuit is negligible (thanks to very high input impedance operational amplifiers), the static estimator equation previously presented in [10] is:

$$\hat{\delta}_s(t) = c_1 V_{out}(t) + c_2 V_{in}(t) - c_3 \int V_{in}(t)dt - Q^*_{DA}(V_{in}, t) \quad (1)$$

where coefficients c_i depend on the physical and geometrical characteristics of the piezocantilever and on the electronic circuit elements: c_1 is related to the ratio between displacement and output voltage, c_2 is a parameter related to an optional reference capacitor in the circuit [10] and c_3 offsets the circuit and actuator leaking currents. Term $Q^*_{DA}(s)$ is the dielectric absorption and is given by:

$$Q^*_{DA}(s) = \frac{k}{\tau s + 1} V_{in}(s) \quad (2)$$

where k and τ are related to static gain and a time constant. The exact steps for identification of self-sensing parameters c_i, τ and k are not described here as are well detailed in [9].

C. Need of dynamic self-sensing

The self-sensing described by Fig.2 and Eq. (1) fits for static and limited bandwidth functioning (see Fig.3). Indeed, $\hat{\delta}_s$ was designed to estimate the steady state value of the displacement δ for a long duration of time (up to 600s). As a result, the transfer between the output $\hat{\delta}_s$ and the input V_{in}, is static and does not account the transient part. Such a model is not convenient for fast closed-loop controller design. To reach the required performances in micromanipulation and microassembly contexts (high accuracy, low response time, disturbance rejection), a dynamic model that accounts the transient part should be used. In parallel, the measurement system (here, the self-sensing) should have a large bandwidth corresponding to the actuator bandwidth performances expected in closed-loop.

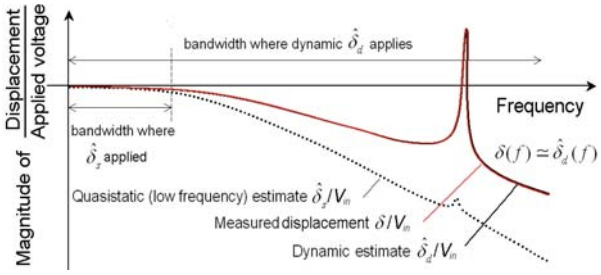

Figure 3. Static (low frequency) [10] and required dynamic self-sensing intended to superpose real (externally measured) displacement.

The next section aims to the extension of the previous self-sensing technique to dynamic self-sensing.

III. EXTENSION TO DYNAMIC SELF-SENSING

A. Principle

The principle of the dynamic self-sensing also relies on the use of V_{in} and V_{out} to estimate the deflection of the piezocantilever. A dynamic part is to be added in cascade with the previous static estimator, as illustrated in fig.4 and detailed in section III.B. The main objective is the computation of the dynamic part gains such that the equality condition between estimated and measured transfer functions holds for both transient and quasistatic parts:

$$\hat{\delta}_d(t) \cong \delta(t); \quad \forall t \quad (3)$$

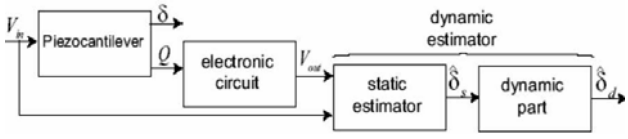

Figure 4. Principle scheme of the dynamic self-sensing technique.

B. Equation of the dynamic part of the estimator

First, we have to compute the transfer function between $\hat{\delta}_s$ and V_{in}. We shall consider an internal transfer function from V_{out} to V_{in}:

$$V_{out}(s) = H(s)V_{in}(s) \qquad (4)$$

Applying the Laplace transformation to Eq. (1) and using Eq. (2) and Eq. (4), we obtain:

$$\hat{\delta}_s(s) = \left[c_1 H(s) + c_2 - \frac{c_3}{s} - \frac{k}{\tau s + 1} \right] V_{in}(s) \qquad (5)$$

Let the scheme in Fig.5 be the block diagram of the dynamic part of the estimator. This proposed scheme is the reverse multiplicative form. The advantage of this structure is that it prevents from bi-causality and bi-stability constraints when inverting transfer functions.

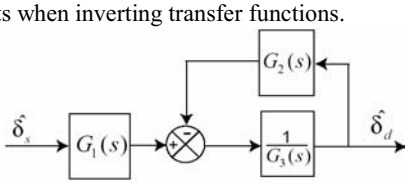

Figure 5. Bloc-scheme of the dynamic part of the estimator.

From Fig.5, we have:

$$\frac{\hat{\delta}_d(s)}{\hat{\delta}_s(s)} = \frac{G_1(s)}{G_2(s) + G_3(s)} . \qquad (6)$$

Using Eq. (5), Eq. (6) and Fig.4, we obtain:

$$\frac{\hat{\delta}_d(s)}{V_{in}(s)} = \left(\frac{G_1}{G_2 + G_3} \right) \left(c_1 H(s) + c_2 - \frac{c_3}{s} - \frac{k}{\tau s + 1} \right) \qquad (7)$$

If approximating with an LTI-model, the mechanical displacement δ of a piezocantilever relative to the applied V_{in} can be characterized by a static gain K and a dynamic part D(s), such as D(s=0) = 1 (see e.g. [4]):

$$\frac{\delta(s)}{V_{in}(s)} = K.D(s) \qquad (8)$$

Using Eq.(7) and Eq.(8) with the condition Eq.(3) we get:

$$\frac{G_1(s)}{G_2(s) + G_3(s)} = \frac{K.D(s)}{c_1 H(s) + c_2 - \frac{c_3}{s} - \frac{k}{\tau s + 1}} \qquad (9)$$

Finally, we can define the different gains of the dynamic part of Eq.(6), as follows:

$$\begin{cases} G_1(s) = K.D(s) \\ G_2(s) = c_1 H(s) - \dfrac{c_3}{s} - \dfrac{k}{\tau s + 1} \\ G_3(s) = c_2 \end{cases} \qquad (10)$$

This result confirms that there is no need to inverse the transfer functions in the proposed dynamic part scheme (Fig.5). Indeed, c_2 is a non-zero real number and, there is no condition of bi-stability required for the models D(s) and/or H(s) such as required for other measurement techniques [6].

Consequently, the parameters are first identified and the proposed dynamic self-sensing is implemented. Finally, a sensorless control using dynamic self-sensing is shown.

C. Experimental setup and results

Fig.6.a depicts the experimental setup. The unimorph piezocantilever is based on a Nickel-layer and a PZT ceramic layer, whose total dimensions are: $15 \times 2 \times 0.3 mm^3$. The electronic circuit shown in Fig.6.b is based on operational amplifiers and we refer the readers to reference [10] for more details. A laser sensor (from Keyence, Fig.6.c) with $100nm$ of accuracy is used to measure the displacement for parameter identification and validation. A computer, a dSPACE real-time controller board and the Matlab-Simulink© software are used to acquire the data, to implement the estimator and to control the piezocantilever.

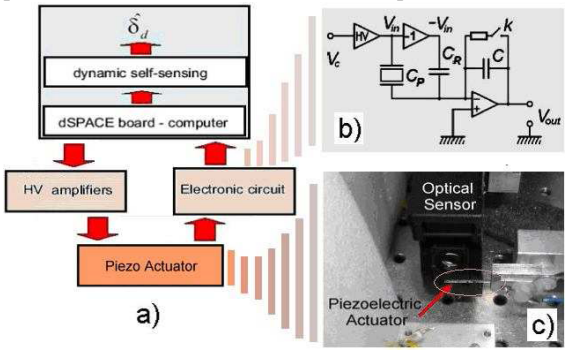

Figure 6. a) Block scheme of experimental setup, b) electronic circuit [10] , c) image of the piezoelectric actuator and of the Keyence sensor (which takes only an evaluation purpose in the system)

The parameters included in Eq. (1)-Eq. (3) are first identified following the procedures in [10]. For the given actuator we identified and calculated: c_1= -3.66µm/V, c_2= 0 µm/V, c_3= $3.4 \cdot 10^{-4}$µmV^{-1}s^{-1}, k= -0.028 µm/V, τ= 60s.

The sampling time in the experiments is 50µs.

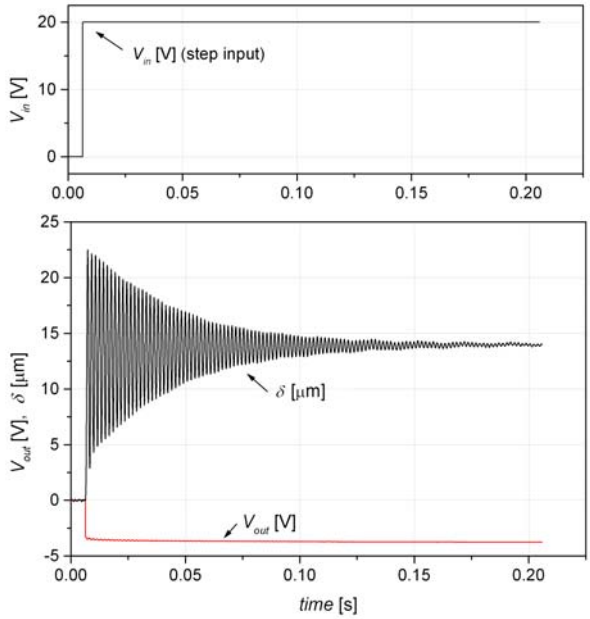

Figure 7. Step response of the piezocantilever measured with the optical sensor (δ) and of the electronic circuit (V_{out}).

Afterwards, to identify K and $D(s)$ of Eq. (6), we apply a step voltage $V_{in}(t)$ and capture the output $\delta(t)$ thanks to the optical sensor (Fig.7). An ARMAX model is derived:

$$\begin{cases} K = 0.690\left[\dfrac{\mu m}{V}\right] \\ D(s) = \dfrac{5.752\times10^{-3}\left(s+3.062\times10^{4}\right)\left(s^{2}-1.95\times10^{4}s+3.076\times10^{8}\right)}{\left(s+3976\right)\left(s^{2}+54.37s+1.362\times10^{7}\right)} \end{cases} \quad (11)$$

In parallel to the measurement of $\delta(t)$ for the identification of D(s) and K, the output V_{out} is also captured. Therefore, using Eq.(4) and the ARMAX method, we also identify the transfer H(s). We obtain:

$$H(s) = \frac{-0.1584\left(s+5.911\times10^{4}\right)\left(s+236.2\right)\left(s+13.74\right)}{\left(s+5.541\times10^{4}\right)\left(s+224\right)\left(s+12.99\right)} \quad (12)$$

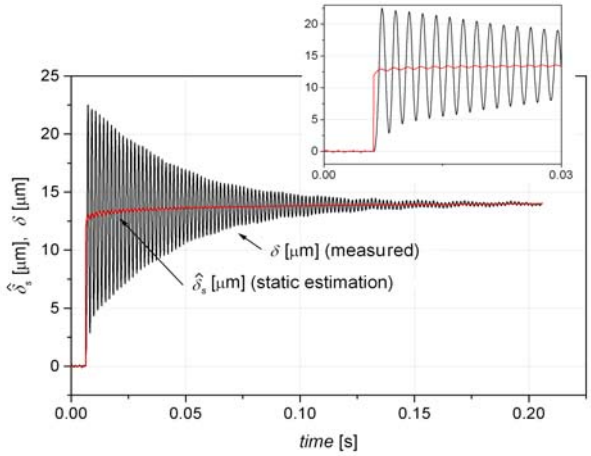

Figure 8. Result with static self-sensing (step input of 20V).

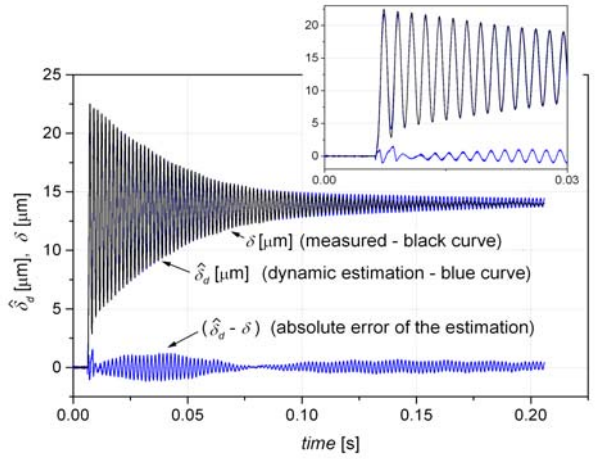

Figure 9. Result with dynamic self-sensing.

Finally, after identification, the gains of the dynamic estimator described by Eq. (10) are computed. Then, the dynamic self-sensing technique (see Fig.4) is implemented. In order to prove its efficiency, both static and dynamic self-sensing techniques were tested and compared. Fig.8 shows the measured displacement and the estimated one for a step input voltage when using the static self-sensing only. It mainly shows that the transient part of the signal is altered while the steady-state value well fits.

Fig.9 shows the measured displacement and the estimate when the dynamic self-sensing technique is used. It demonstrates that the estimate fits well the real displacement both in transient and in steady-state parts.

IV. CONTROL OF THE DISPLACEMENT

In this section, we use the proposed dynamic self-sensing to a control application. It should be noted that measured displacement δ given by the optical sensor is only shown for evaluation purposes and does not serve as closed loop reference.

A. System to be controlled

As we can see in the previous results (Fig. 9), the piezocantilever is very resonant (more than 64% of overshoot). Such a behavior is undesirable in micromanipulation and microassembly tasks because the piezocantilever, that is often a part of a microgripper, may destroy the manipulated micro-object or conversely the latter can destroy the former. Furthermore, microrobots are generally very sensitive to external disturbances (temperature, ambient vibrations, etc.). In order to reject the effects of these disturbances, a closed-loop control is required. For that, we will use the measurement (estimation) of the displacement through the self-sensing.

In this section, we design a controller for the piezocantilever. The robust H_∞ synthesis technique has been chosen because of the possibility to account a priori specifications (performances and disturbance rejection) and because of its robustness relative to eventual model uncertainty. Fig.10 presents the system to be controlled. It contains the piezocantilever and the dynamic self-sensing circuit (electronic circuit, static estimator and dynamic part). While the input is V_{in}, the output that will be used for the feedback is the estimate $\hat{\delta}_d$. Concerning the real output δ, there may be an eventual external disturbance d (manipulation force, temperature effect, etc.). Because the charges Q appearing on the electrodes directly depend on the displacement δ, and because $\hat{\delta}_d$ comes from these measured charges, the influence of the disturbance d is also detected by the estimate $\hat{\delta}_d$, i.e. $\hat{\delta}_d(t) = \delta(t)$ whatever d is. Therefore, the rejection of the effect of d is possible even if we use $\hat{\delta}_d$ for the feedback control.

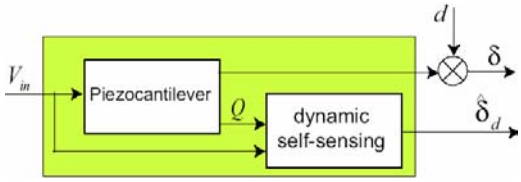

Figure 10. Block diagram of dynamic self-sensing.

B. Specifications

Microassembly systems generally require micrometer accuracy notably for motion generation, gripping and feeding tasks. Furthermore, in most of cases, the behavior of piezocantilevers used in microassembly and micromanipulation is desired to be without (or only with a very small one) overshoot. This notably enables ensuring better quality tasks. It is also interesting to limit the applied voltage and to guarantee the rejection of disturbances. Thus, we consider the following specifications:

Performances: the overshoot, which was initially 64% as pictured in Fig.9, should be cancelled.

Limitation of the voltage: the applied voltage V_{in} should be limited in order to avoid permanent damage on the piezocantilever. We choose a maximal ratio of $\frac{V_{in}^{\max}}{\delta_{\max}} = \frac{100[V]}{20[\mu m]} = 5\ \mathrm{V}/\mu\mathrm{m}$, where $\delta_{\max}$ corresponds to the maximal range of use.

Disturbance rejection: the disturbance to be rejected is mainly the temperature effects. We use: $\frac{\delta}{\Delta T}(s=0) = \frac{1\mu m}{10°C}$.

C. H_∞ controller synthesis

As described above, one of the interests of the H_∞ synthesis is the explicit account of the specifications. These specifications are transcribed into weighting functions during the synthesis.

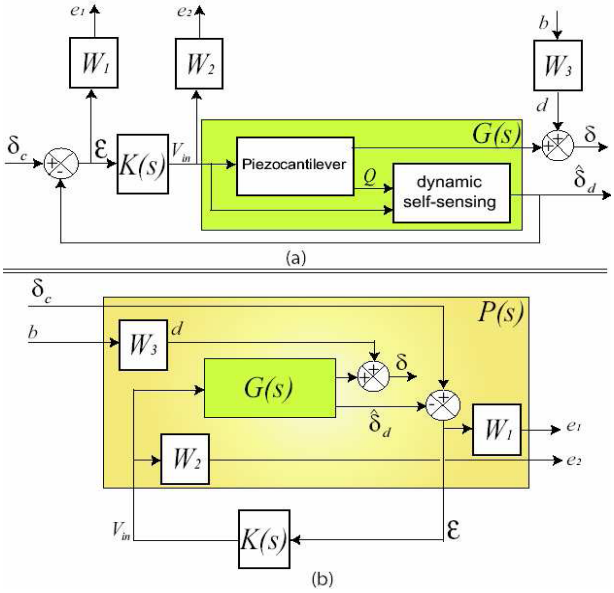

Figure 11. (a): The closed-loop scheme with the weighting functions. (b): The equivalent standard scheme.

Let Fig.11-a present the closed-loop scheme for the controller design, where the weighting functions W_1, W_2 and W_3 are used to include the specifications. From this figure:

$$\begin{cases} e_1 = W_1 S\delta_c - W_1 S W_3 b \\ e_2 = W_2 KS\delta_c - W_2 KSW_3 b \end{cases} \quad (13)$$

where $S = (1+KG)^{-1}$ is the sensitivity function.

Using the standard form pictured in Fig.11-b and applying the H_∞ standard problem [12] to Eq. (13), we obtain the following optimization problem:

$$\left\| \begin{matrix} W_1 \cdot S \\ W_1 \cdot S \cdot W_3 \\ W_2 \cdot K \cdot S \\ W_2 \cdot K \cdot S \cdot W_3 \end{matrix} \right\|_\infty < \gamma \Rightarrow \begin{matrix} |S| < \frac{\gamma}{|W_1|} & |KS| < \frac{\gamma}{|W_2|} \\ |S| < \frac{\gamma}{|W_1 \cdot W_3|} & |KS| < \frac{\gamma}{|W_2 \cdot W_3|} \end{matrix} \quad (14)$$

where the aim consists in finding an optimal value $\gamma > 0$ and a controller $K(s)$.

To solve the problem of Eq. (14), we use the Glover-Doyle algorithm that is based on the Riccati equations [13][14].

D. Computation of the controller

The weighting functions were chosen accordingly to the specifications. So, we choose the following set:

$$W_1 = \frac{0.005s+1}{s+0.001},\ W_2 = \frac{2\times10^{-5}s+1}{6.25\times10^{-5}s+5} \text{ and } W_3 = 0.01 \quad (15)$$

The computed controller has an order of 7. Such an order is too high and may lead to time consuming and sometimes to instability of the closed-loop. So, we decide to reduce the controller order using the balanced realization technique [15]. Finally, we obtain:

$$\begin{cases} K = \dfrac{1.547s + 4.765\times10^4}{s^2 + 504s + 0.503} \\ \gamma_{opt} = 0.63 \end{cases} \quad (16)$$

γ_{opt} being smaller than 1 indicates that the controller will ensure the performances described in the specifications (section *IV.B*)

E. Experimental results

The first experiment consists in applying a series of step reference to the closed-loop system. Alternatively, the optical displacement measurement is used only to validate the estimation and the control results. The results, given in Fig.12, show that the vibration was completely removed. Furthermore, it shows that the estimated displacement $\hat{\delta}_d$ well fits to the real displacement δ (measured with the optical sensor), with a short-term accuracy lower than 2%.

In the second experiment, we apply arbitrary levels of reference input (Fig.13). Self sensing control is performed over an extended period of 300 seconds, which is largely sufficient for most micropositioning/micromanipulation tasks. The objective is to evaluate the input voltage V_{in}. As presented in Fig.13b, when the step reference is equal to the maximal range of use ($-8\mu m \rightarrow 8\mu m$), the applied voltage is largely inferior (ΔV_{in} ; $45V$) to the limit imposed in the specifications (100V).

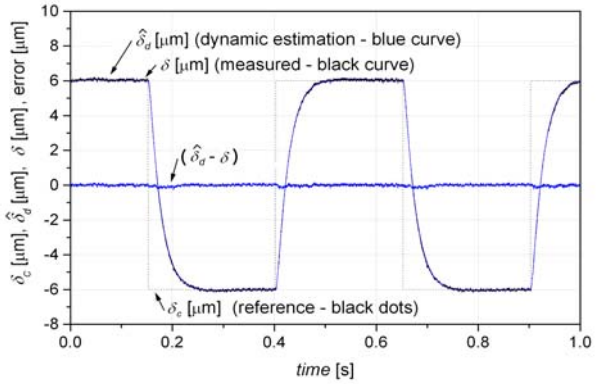

Figure 12. Step response of the closed-loop system.

Summarizing, the recorded maximum error from Fig.13 is 0.4 µm, which, reported to the reference signal, represents a fair 5% for the combined short-term and long-term experiments.

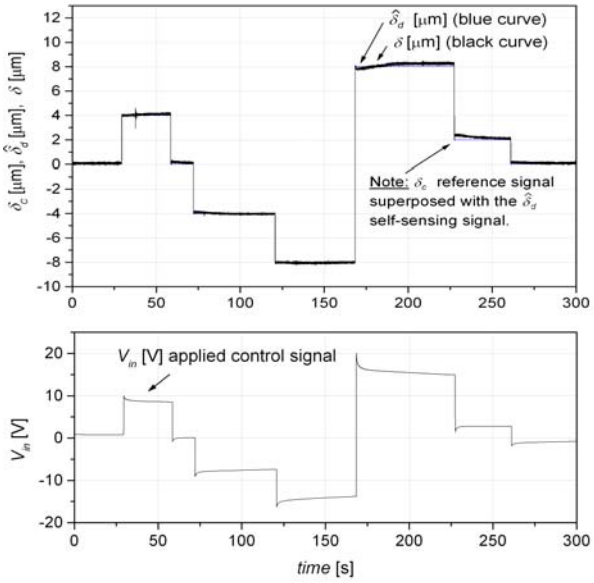

Figure 13. Complete and long term response of the closed-loop system.

V. Conclusion

In this paper, a dynamic self-sensing technique is proposed for piezoelectric actuators. Afterwards, the issued estimated displacement is used in a closed-loop control based on a robust H_∞ controller.

The principle of the proposed dynamic self-sensing technique is based on a previous static self-sensing scheme that we extended by adding a dynamic part. The aim is to estimate the displacement of the piezoelectric actuator both in the transient and in the steady-state modes through the measured charges. Analytical solutions are given to compute the gains of the additive dynamic part in order to help the users. The usefulness of the dynamic self-sensing technique was demonstrated in a closed-loop control scheme. The controller was computed using the robust H_∞ synthesis in order to ensure performances required in the micromanipulation and microassembly context. The experimental results demonstrate the sub-micrometer accuracy of the proposed self-sensing scheme, both on transient and steady-state modes, and its efficiency for closed-loop control applications.

The proposed solution brings a cost effective (no external sensors), compact and accurate device for microrobotic and microassembly applications. Moreover, such an approach could also enable the environmental variations compensations (among them temperature), which are usually influent for applications where a high accuracy is required.

References

[1] D. Tolfree and M. J. Jackson, Commercializing Micro-Nanotechnology Products. CRC Press. 2006

[2] R. Pérez, J. Agnus, C. Clévy, A. Hubert, N. Chaillet, *Modelling, fabrication and validation of a high performance 2 DOF*, IEEE/ASME Transactions on Mechatronics, vol. 10, N°2, april 2005.

[3] M. Rakotondrabe, C. Clévy and P. Lutz, *Complete open loop control of hysteretic, creeped and oscillating piezoelectric cantilever*, IEEE – Trans. on Automation Science and Engineering (T-ASE), in press.

[4] M. Rakotondrabe, C. Clévy and P. Lutz, *Modelling and robust position/force control of a piezoelectric microgripper*, IEEE - CASE, (International Conference on Automation Science and Engineering), pp:39-44, Scottsdale AZ USA, Sept 2007.

[5] B. Borovic and A. Q. Liu and D. Popa and H. Cai and F. L. Lewis, *Open-loop versus closed-loop control of MEMS devices: choices and issues*, Journal of Micromechechanics and Microengineering, Vol.15, N°10, pp.1917-1924, 2005.

[6] M. Rakotondrabe, Y. Haddab and P. Lutz, *Nonlinear modelling and estimation of force in a piezoelectric cantilever*, IEEE/ASME - AIM, (International Conference on Advanced Intelligent Mechatronics), Zurich Switzerland, Sept 2007.

[7] A.J. Fleming and S.O.R. Moheimani, *Control oriented synthesis of high performance piezoelectric shunt impedances for structural vibration control*, IEEE Transactions on Control Systems Technology 13(1), pp 98-112, 2005.

[8] Y. Cui, *Self-Sensing Compounding Control of Piezoceramic Micro-Motion Worktable Based on Integrator*, Proc. to 6th World Congress on Intell. Cont. and Autom., China, 2006

[9] A. S. Putra, H. Sunan, T. K. Kok, S.K. Panda and T. H. Lee, *Self-Sensing Actuation With Adaptive Control in Applications With Switching Trajectory*, IEEE/ASME Trans. on Mechatronics, vol. 13, no. 1, pp. 104-110, 2008

[10] I. A. Ivan, M. Rakotondrabe, P. Lutz and N. Chaillet, *Quasi-static displacement self-sensing method for cantilevered piezoelectric actuators*, Review of Scientific Instruments (RSI), Vol.80(6), 065102, June 2009.

[11] I. A. Ivan, M. Rakotondrabe, P. Lutz and N. Chaillet, *Current integration force and displacement self-sensing method for cantilevered piezoelectric actuators*, Review of Scientific Instruments (RSI), Vol.80(12), 2126103, December 2009.

[12] G. J. Balas, J. C. Doyle, K. Glover, A. Packard and R. Smith, *µ-synthesis and synthesis toolbox*, The Mathworks User's Guide-3, 2001.

[13] K. Glover and J. C. Doyle, *State-space formulae for all stabilizing controllers that satisfy an H-inf norm bound and relations to risk sensitivity*, Systems & Control Letters 11, 1988.

[14] J. C. Doyle, K. Glover, P. K. Khargonekar and B. A. Francis, *State-space solutions to standards H2 and H-inf control problems*, IEEE Transactions on Automatic Control, AC 34 No8, 1989.

[15] B. C. Moore, Principal component analysis in linear systems, IEEE Transactions on Automatic Control, AC-26(1), 1981.